H II Regions: Witnesses to Massive Star Formation

Thomas Peters

Institut für Theoretische Astrophysik
Zentrum für Astronomie der Universität Heidelberg

Ralf Klessen, Robi Banerjee (ITA, Heidelberg),
Mordecai-Mark Mac Low (AMNH, New York),
Roberto Galván-Madrid, Eric Keto (CfA, Harvard),
Cornelis Dullemond (MPIA, Heidelberg)

Simulations Summary

Simulating radiation feedback from massive stars

- adaptive-mesh numerical hydrodynamics code FLASH
- raytracing algorithm for ionizing and non-ionizing radiation
- rate equation for ionization fraction
- relevant heating and cooling processes
- sink particles as sources of radiation
- simple prestellar model

We try to understand

- the formation of massive stars,
- the role of radiative feedback in stellar cluster formation,
- morphologies and kinematics of ultracompact H II regions.

Initial Conditions

- massive core with $M = 1000 M_{\odot}$
- flat core within $r = 0.5\,\mathrm{pc}$ and $\rho(r) \sim r^{-3/2}$ density fall-off
- core is initially rotating with $\beta = 0.05$
- no magnetic fields or turbulence
- sink particle radius is $590\,\mathrm{AU}$
- cut-off density is $7 \cdot 10^{-16}\,\mathrm{g\,cm^{-3}}$
- cell size is $98\,\mathrm{AU}$

Classification of UC H II Regions

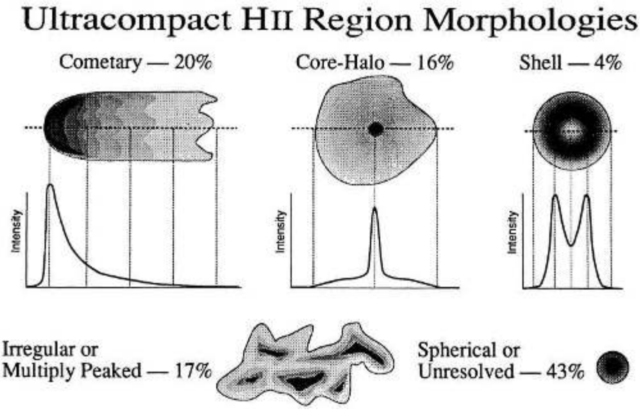

- Wood & Churchwell 1989 classification of UC H II regions
- Question: What is the origin of these morphologies?
- UC H II lifetime problem: Too many UC H II regions observed!

H II Region Morphologies

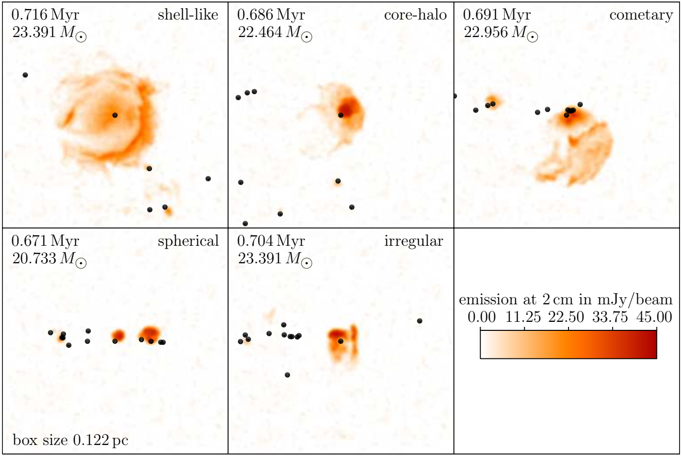

- synthetic VLA observations at $2\,\mathrm{cm}$ of simulation data
- interaction of ionizing radiation with accretion flow creates high variability in time and shape
- a single simulation reproduces all H II region morphologies

H II Region Morphologies

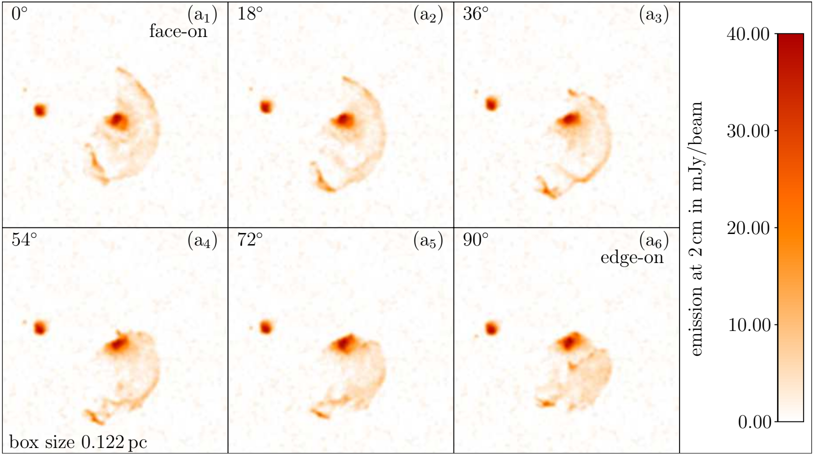

- morphologies depend a lot on viewing angle
- example: shell morphology face-on turns into cometary morphology edge-on
- different behavior in each particular case

H II Region Morphologies

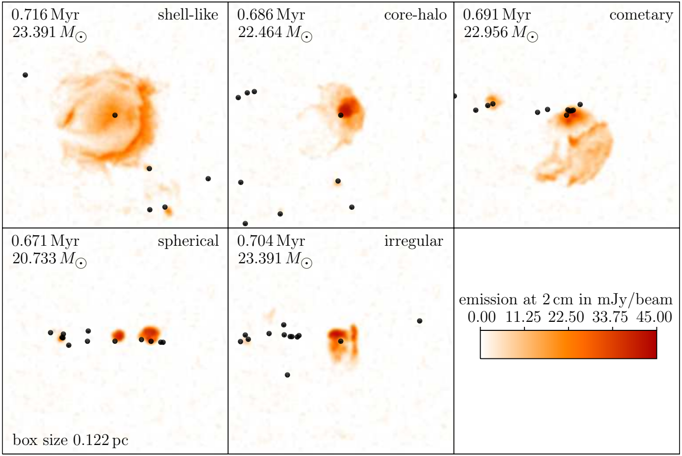

- infalling gas shields ionizing radiation, ionized gas recombines
- as long as the massive star is embedded in an accretion flow, the H II region cannot expand freely
- H II region flickers, this resolves the lifetime problem!

Time Variability

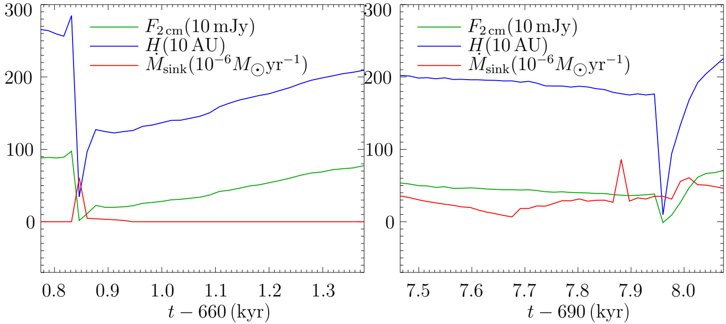

- correlation between accretion events and H II region changes
- time variations in size and flux have been observed
- changes of size and flux of $5\text{–}7\%\mathrm{yr}^{-1}$ match observations

  Franco-Hernández et al. 2004, Rodríguez et al. 2007, Galván-Madrid et al. 2008

Comparison with W51e2

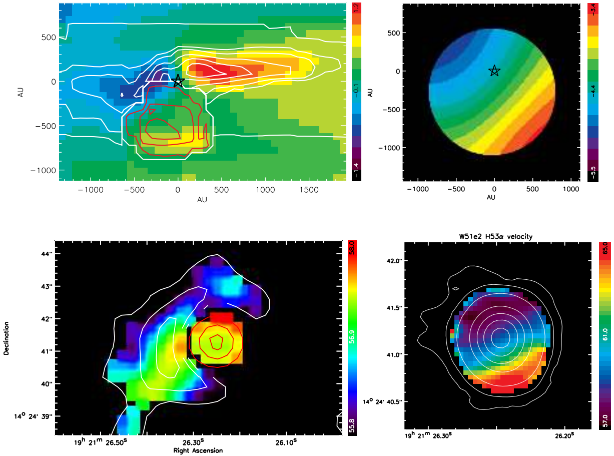

Zhang et al. 98, Keto & Klaassen 08

- synthetic NH_3(3,3) and H53α maps
- H II region offset from central protostar
- ionized gradient indicative of spiralling flow

Conclusions and Outlook

Conclusions

- high variability in time and shape of H II regions
- all classified morpholgies can be found in a single simulation
- flickering resolves the UC H II lifetime problem
- observed size and flux changes are caused by accretion process
- simulations reproduce characteristic H II region features such as spiralling flows

Outlook

- more realistic initial conditions
- study effects of turbulence and magnetic fields
- detailed recombination line (H and Ne II) studies

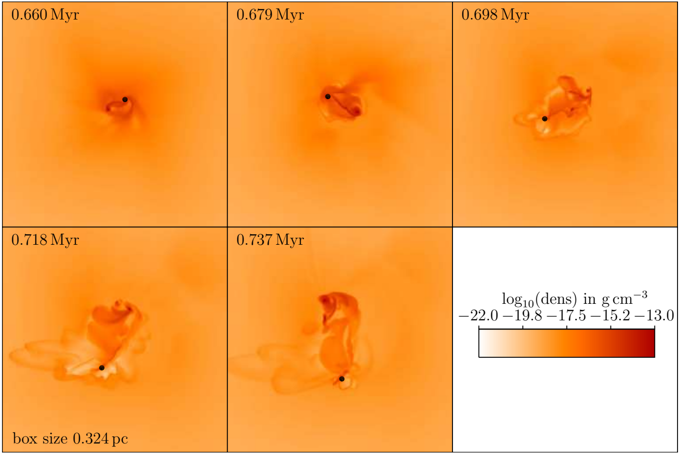

- disk is gravitationally unstable and fragments
- we suppress secondary sink formation by “Jeans heating”
- H II region is shielded effectively by dense filaments
- ionization feedback does not cut off accretion!

Disk Fragmentation

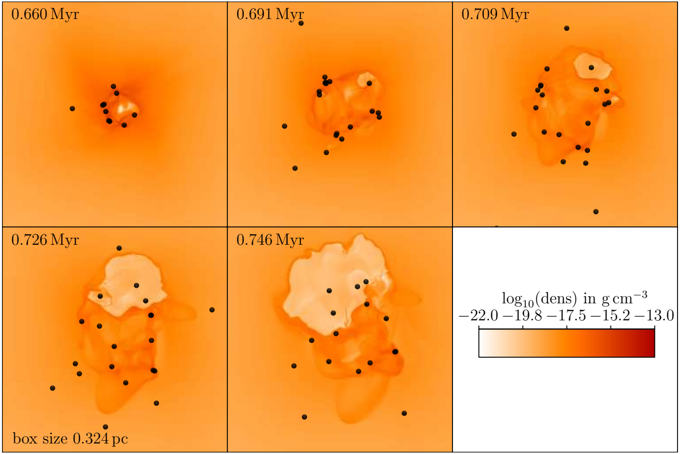

- all protostars accrete from common gas reservoir
- accretion flow suppresses expansion of ionized bubble
- cluster shows "fragmentation-induced starvation"
- halting of accretion flow allows bubble to expand

Accretion History

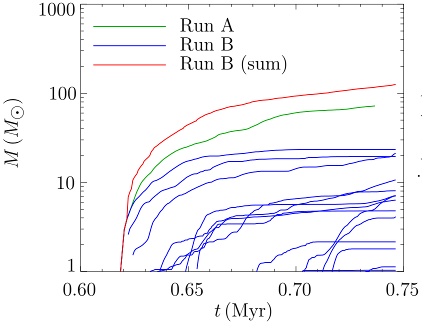

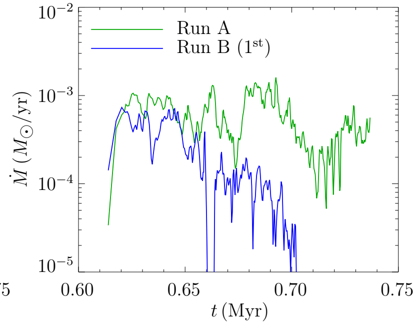

- single protostar accretes $72 M_\odot$ in $120\,\mathrm{kyr}$ (Run A)
- ionization feedback alone is unable to stop accretion
- accretion is limited when multiple protostars can form (Run B)
- no star in multi sink simulation reaches more than $30 M_\odot$

Accretion History

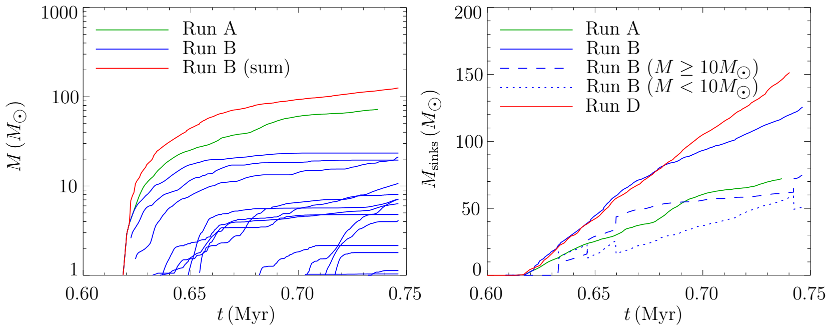

- compare with control run without radiation feedback
- total accretion rate does not change with accretion heating
- expansion of ionized bubble causes turn-off
- no triggered star formation by expanding bubble

Dynamics of the H II Region and Outflow

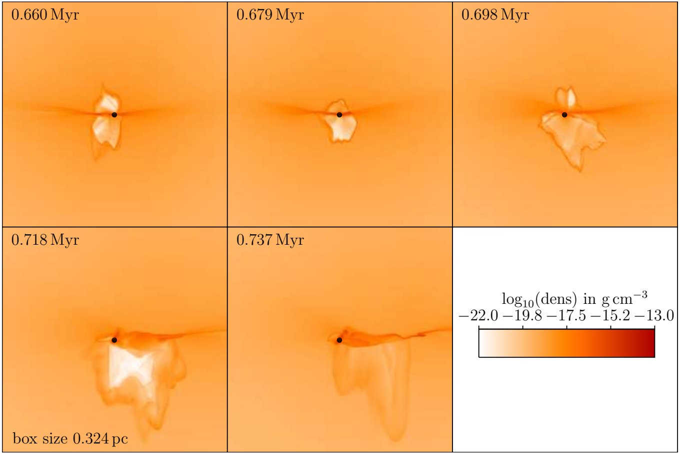

- thermal pressure drives bipolar outflow
- filaments can effectively shield ionizing radiation
- when thermal support gets lost, outflow gets quenched again
- no direct relation between mass of star and size of outflow

Dynamics of the H II Region and Outflow

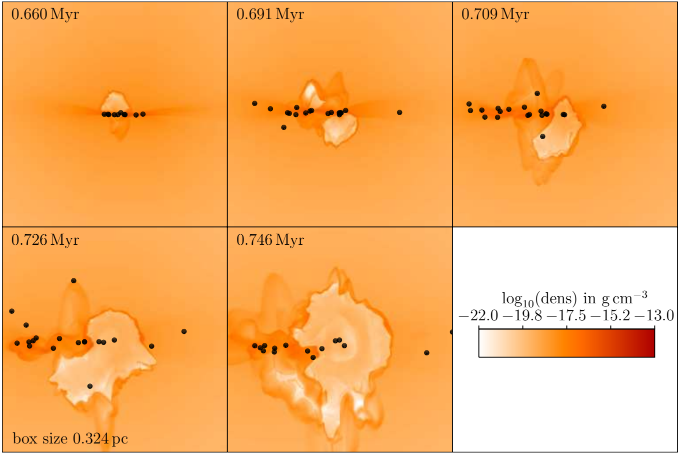

- bipolar outflow during accretion phase
- when accretion flow stops, ionized bubble can expand
- expansion is highly anisotropic
- bubbles around most massive stars merge

Dynamics of the H II Region and Outflow

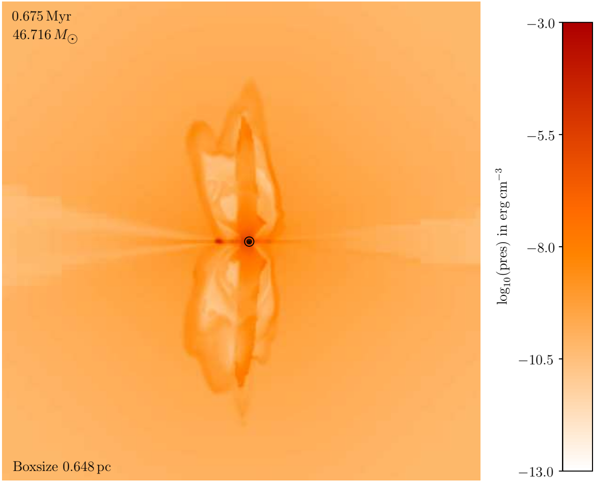

- ionization drives bipolar outflow
- pressure-driven expansion of shell
- thin-shell instability leads to fingers

Dynamics of the H II Region and Outflow

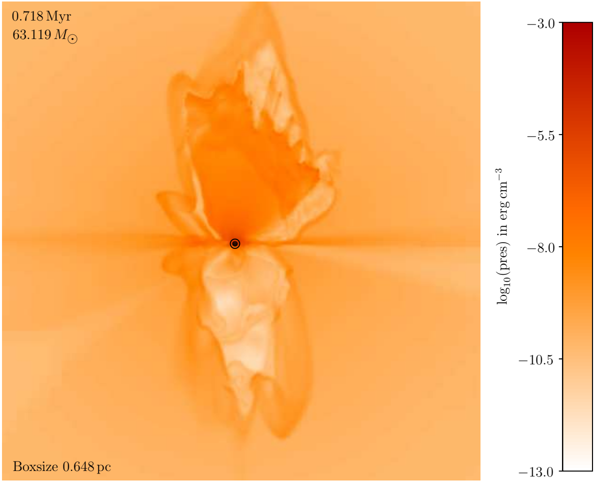

- photoionization hindered by infalling material
- hot gas recombines and cools
- result is a cometary H II region

Dynamics of the H II Region and Outflow

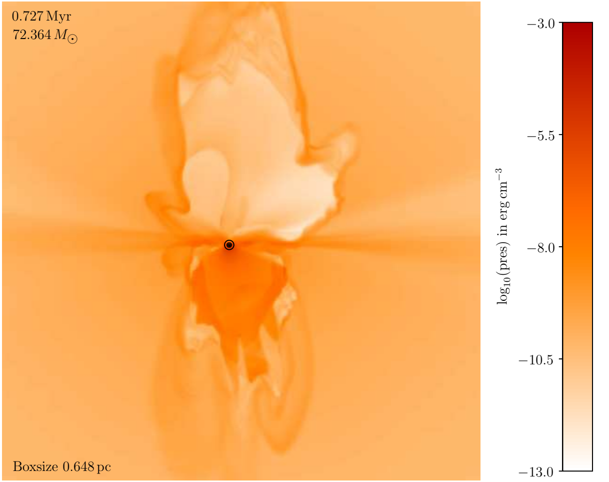

- size and morphology of H II region is highly variable
- cometary H II region totally reverses within less than 10 kyr
- changes like this have been observed!

Simulated Radio Continuum Maps

- numerical data can be used to generate continuum maps
- calculate free-free absorption coefficient for every cell
- integrate radiative transfer equation (neglecting scattering)
- convolve resulting image with beam width
- VLA parameters:
  - distance $2.65\,\mathrm{kpc}$
  - wavelength $2\,\mathrm{cm}$
  - FWHM $0\rlap{.}''14$
  - noise $10^{-3}\,\mathrm{Jy}$

H II Region Morphologies

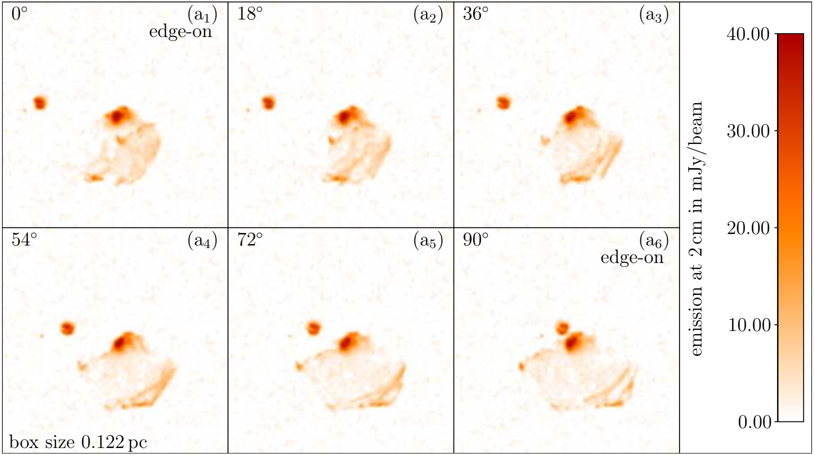

- morphologies depend a lot on viewing angle
- example: shell morphology face-on turns into cometary morphology edge-on
- different behavior in each particular case

H II Region Morphologies

Type	WC89	K94	Run A	Run B
Spherical/Unresolved	43	55	19	60 ± 5
Cometary	20	16	7	10 ± 5
Core-halo	16	9	15	4 ± 2
Shell-like	4	1	3	5 ± 1
Irregular	17	19	57	21 ± 5

WC89: Wood & Churchwell 1989, K94: Kurtz et al. 1994

- statistics over 25 simulation snapshots and 20 viewing angles
- statistics can be used to distinguish between different models
- single sink simulation does not reproduce lifetime problem

Emission and Optical Depth

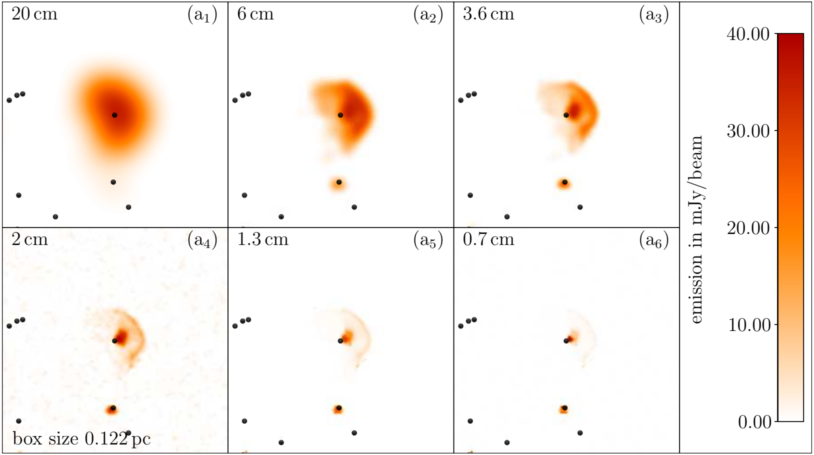

- same H II region for different VLA wavelengths
- beam size and optical depth become smaller with decreasing wavelength

Emission and Optical Depth

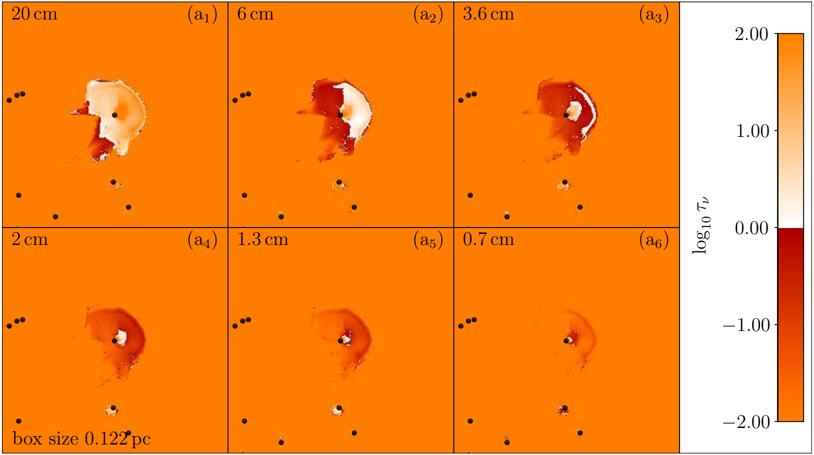

- same H II region for different VLA wavelengths
- beam size and optical depth become smaller with decreasing wavelength

Spectral Energy Distribution

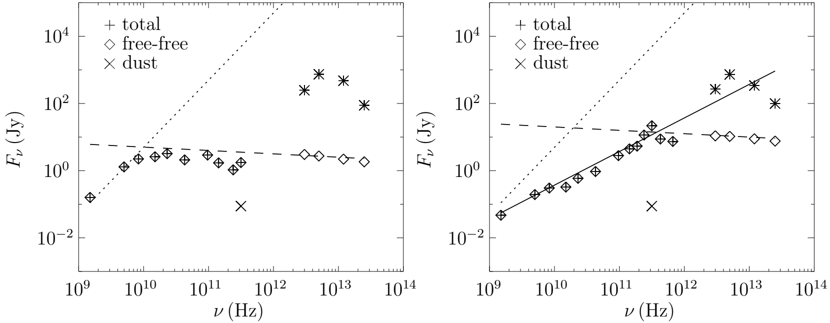

- simulated dust emission with RADMC-3D
- typical H II region SEDs of WC89 reproduced
- expect spectral slope of $\alpha = 2$ (optically thick) and $\alpha = -0.1$ (optically thin)
- anomalous SEDs with $\alpha \approx 1$ caused by density inhomogeneities
- no dust emission in cm to sub-mm regime

Time Variability

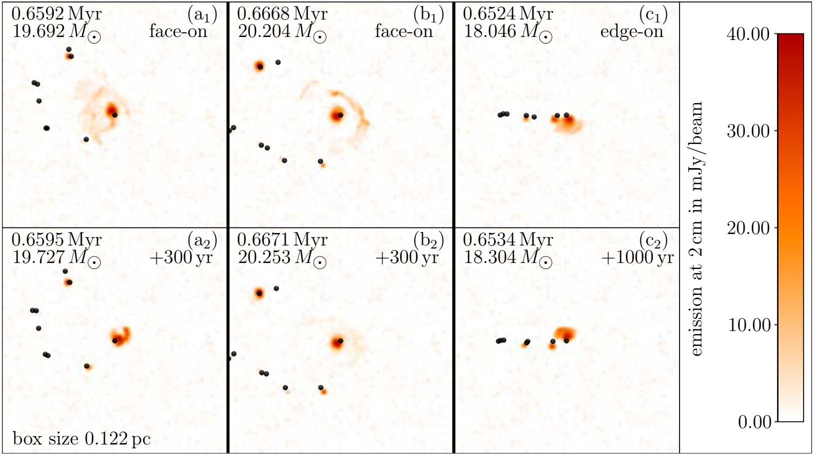

- H II regions can change dramatically in only a few 100 yr.
- shells and filaments can appear and disappear
- cometary H II regions can reverse

Time Variability

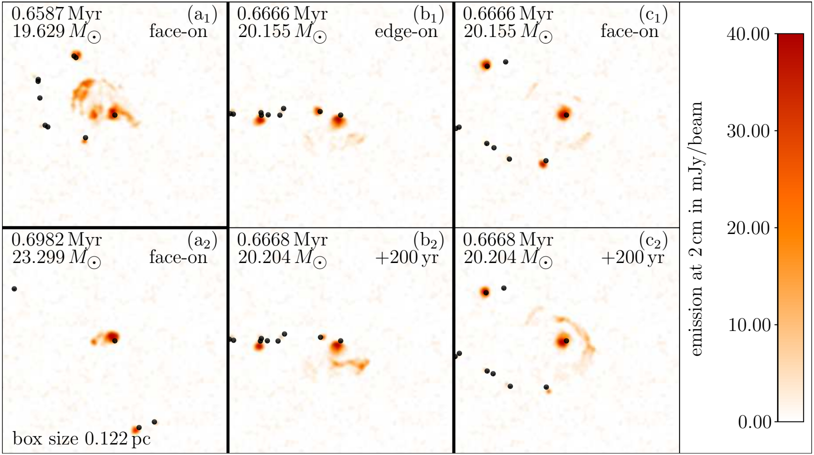

- H II regions can change dramatically in only a few 100 yr.
- shells and filaments can appear and disappear
- cometary H II regions can reverse

Effect of Feedback on Stellar Cluster

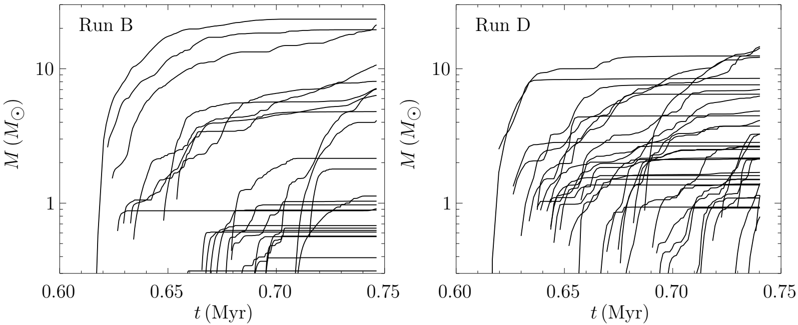

- accretion heating by first stars raises local Jeans mass
- stars become more massive, but less stars form in total
- stars more massive with (Run B) than without (Run D) feedback
- accretion histories of individual stars can vary a lot

Effect of Feedback on Stellar Cluster

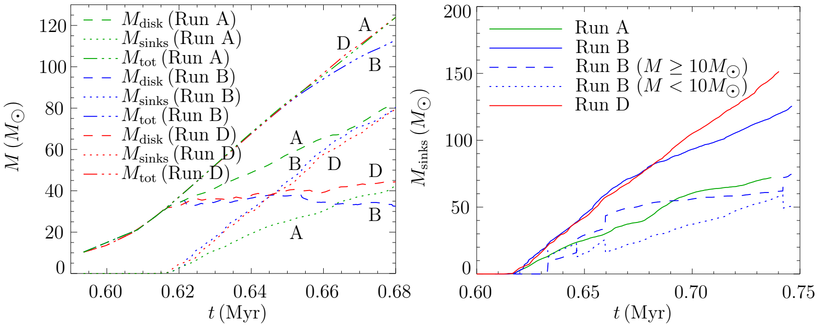

- star formation keeps the disk mass roughly constant
- ionization-driven outflows reduce the disk mass slightly
- ionizing radiation does not change the star formation rate initially

Effect of Feedback on Stellar Cluster

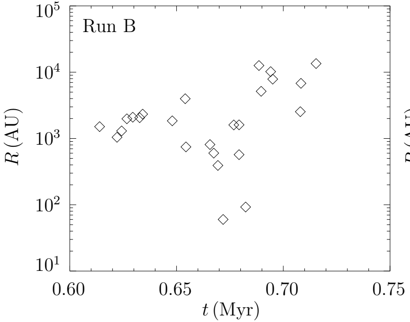

- star formation proceeds radially outwards in disk plane
- accretion heating by first stars suppresses sink formation at small disk radii

Effect of Feedback on Stellar Cluster

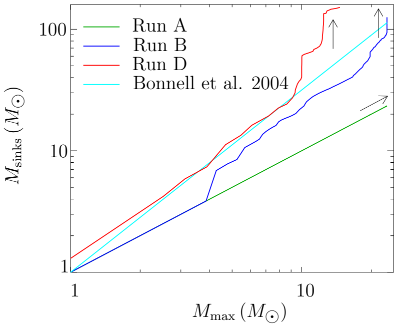

- competitive accretion simulations and observations show a relation $M_{\rm max} \propto M_{\rm sinks}^{2/3}$
- fragmentation-induced starvation can equally well reproduce this scaling relation
- accretion heating shifts the turn-off towards higher masses

Jeans Heating

- to study effect of single ionizing source, artificial fragmentation must be suppressed
- if gas density gets too high, the Jeans length is no longer resolved
- instead of forming secondary sink particles, we heat up the gas such that we resolve the Jeans length

$$T_{\rm min} = \frac{G \mu m_{\rm p}}{\pi k_{\rm B}} \rho (n \Delta x)^2$$

Raytracing Module

Long Characteristics

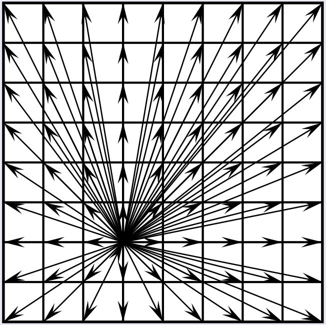

- pro:
  very accurate,
  fully parallelizable
- con:
  redundant calculations

Raytracing Module

Long Characteristics

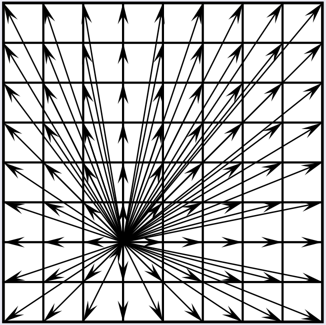

- pro:
  very accurate,
  fully parallelizable
- con:
  redundant calculations

Short Characteristics

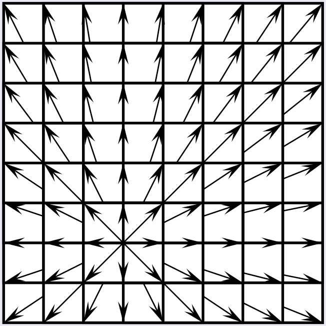

- pro:
  very efficient
- con:
  need for interpolation,
  intrinsically serial

Raytracing Module

Hybrid Characteristics (Rijkhorst et al. 2006)

- computational domain is distributed over several processors
- use long characteristics on every single patch
- use long characteristics again to add up contributions of different patches

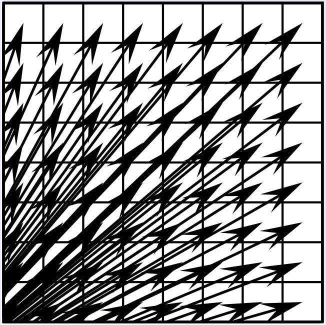

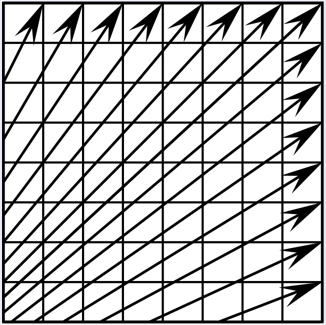

Radiation Physics

- raytracing yields optical depths for ionizing and non-ionizing radiation
- local mean intensity is given by

$$J_\nu(r) = \left(\frac{r_{\rm star}}{r}\right)^2 \frac{1}{2c^2} \frac{h\nu^3}{\exp(h\nu/k_{\rm B}T_{\rm star}) - 1} \exp(-\tau_\nu(r))$$

- input for photoionization rate and photoionization heating rate

Change of Ionization Fraction

- rate equation for hydrogen

$$\frac{\mathrm{d}x(\mathrm{HII})}{\mathrm{d}t} = x(\mathrm{HI})(A_\mathrm{p} + A_\mathrm{c}) - x(\mathrm{HII}) n_\mathrm{e} \alpha_\mathrm{R}$$

- photoionization rate

$$A_\mathrm{p} = \int_{\nu_0}^{\infty} \frac{4\pi J_\nu}{h\nu} a_\nu \, \mathrm{d}\nu$$

- collisional ionization rate

$$A_\mathrm{c} = A_\mathrm{c}(\mathrm{HI}) n_\mathrm{e} \sqrt{T} \exp(-I(\mathrm{HI})/k_\mathrm{B} T)$$

- radiative recombination rate

$$\alpha_\mathrm{R} = \alpha_\mathrm{R}(10^4\,\mathrm{K}) \left(\frac{T}{10^4\,\mathrm{K}} \right)^{-0.7}$$

Change of Ionization Fraction

- rate equation for hydrogen

$$\frac{\mathrm{d}x(\mathrm{HII})}{\mathrm{d}t} = x(\mathrm{HI})(A_\mathrm{p} + A_\mathrm{c}) - x(\mathrm{HII}) n_\mathrm{e} \alpha_\mathrm{R}$$

- photoionization rate

$$A_\mathrm{p} = \int_{\nu_0}^{\infty} \frac{4\pi J_\nu}{h\nu} a_\nu \, \mathrm{d}\nu$$

- collisional ionization rate

$$A_\mathrm{c} = A_\mathrm{c}(\mathrm{HI}) n_\mathrm{e} \sqrt{T} \exp(-I(\mathrm{HI})/k_\mathrm{B} T)$$

- radiative recombination rate

$$\alpha_\mathrm{R} = \alpha_\mathrm{R}(10^4\,\mathrm{K}) \left(\frac{T}{10^4\,\mathrm{K}} \right)^{-0.7}$$

Change of Temperature

- photoionization heating rate:

$$\Gamma_{\mathrm{p}} = n(\mathrm{HI}) \int_{\nu_0}^{\infty} \frac{4\pi J_\nu}{h\nu} a_\nu h(\nu - \nu_0)\,\mathrm{d}\nu$$

- high temperature (metal line) cooling curve

Change of Temperature

- photoionization heating rate:

$$\Gamma_{\mathrm{p}} = n(\mathrm{HI}) \int_{\nu_0}^{\infty} \frac{4\pi J_\nu}{h\nu} a_\nu h(\nu - \nu_0)\, \mathrm{d}\nu$$

- high temperature (metal line) cooling curve

Conclusion

- sensitive interdepedence of x and T
- use sub-cycling with thermal time scale
- iterate until x and T converge
- implementation from DORIC routines (Rijkhorst et al. 2006)

- code was tested in cosmological setting by Iliev et al. 2006
- for our interests, D-type ionization fronts need to be modeled
- Spitzer 1978 gives solution for expansion into homogeneous medium

$$R(t) = R_S \left(1 + \frac{7}{4}\frac{c_s t}{R_S}\right)^{4/7}$$

- analytical and numerical results agree very well

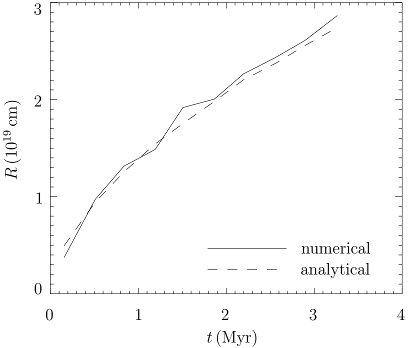

Prestellar Model

Ionizing Radiation

- sink particles as model for protostars
- luminosity and temperature from ZAMS (Paxton 2004)

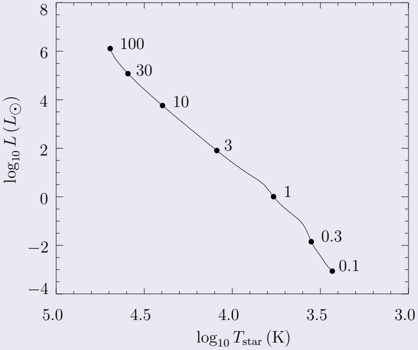

- defines ionizing radiation completely

Prestellar Model

Non-ionizing Radiation

- following Krumholz et al. 2007, the dust heating term to lowest order in v/c is $\Gamma_\mathrm{d} = \kappa_\mathrm{P} \rho c u$
- total energy density is given by

$$u(r) = \left(\frac{r_\mathrm{star}}{r}\right)^2 \frac{\sigma}{c} \exp(-\tau(r)) T_\mathrm{star}^4$$

- stellar heating term is

$$\Gamma_\mathrm{st}(r) = \sigma \left(\frac{r_\mathrm{star}}{r}\right)^2 \kappa_\mathrm{P}(T(r)) \rho(r) \exp(-\tau(r)) T_\mathrm{star}^4$$

Prestellar Model

Accretion Luminosity

- assume that potential energy is fully converted into radiation at accretion radius

$$L_{\mathrm{acc}} = G \frac{M \dot{M}}{r_{\mathrm{acc}}}$$

- prestellar evolution model from Hosokawa & Omukai 2008
- interpolate to find r_{acc} as function of M and $\dot{M}$
- additional heating term

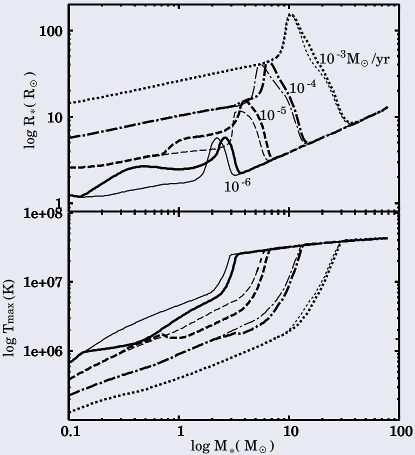

$$\Gamma_{\mathrm{acc}}(r) = \sigma \left(\frac{r_{\mathrm{acc}}}{r} \right)^2 \kappa_{\mathrm{P}}(T(r)) \rho(r) \exp(-\tau(r)) T_{\mathrm{acc}}^4$$

Summary

Full Euler Equations

$$\partial_t \rho + \nabla \cdot (\rho \boldsymbol{v}) = 0$$

$$\partial_t (\rho \boldsymbol{v}) + \nabla \cdot (\rho \boldsymbol{v} \otimes \boldsymbol{v}) + \nabla P = \rho \boldsymbol{g}$$

$$\partial_t (\rho e_{\mathrm{tot}}) + \nabla \cdot [(\rho e_{\mathrm{tot}} + P) \boldsymbol{v}] = \rho \boldsymbol{v} \cdot \boldsymbol{g} + \Gamma - \Lambda$$

with

$$\Gamma = \Gamma_{\mathrm{p}} + \Gamma_{\mathrm{st}} + \Gamma_{\mathrm{acc}}$$

and

$$\Lambda = \Lambda_{\mathrm{ml}} + \Lambda_{\mathrm{mol}} + \Lambda_{\mathrm{gd}}$$

References

Rijkhorst et al. 2006, Banerjee et al. 2006, Federrath et al. 2010, Peters et al. 2010